IEEE Access
Multidisciplinary ⋮ Rapid Review ⋮ Open Access Journal

Received October 16, 2020, accepted November 2, 2020, date of publication November 6, 2020, date of current version November 19, 2020.

Digital Object Identifier 10.1109/ACCESS.2020.3036381

Transmission Expansion Planning Model Considering Battery Energy Storage, TCSC and Lines Using AC OPF

ZORA LUBURIĆ[1], (Member, IEEE), HRVOJE PANDŽIĆ[2,3], (Senior Member, IEEE), AND MIGUEL CARRIÓN[4], (Member, IEEE)

[1]Croatian Transmission System Operator-HOPS, 10000 Zagreb, Croatia
[2]Innovation Centre Nikola Tesla, 10000 Zagreb, Croatia
[3]Faculty of Electrical Engineering and Computing, University of Zagreb, 10000 Zagreb, Croatia
[4]School of Industrial and Aerospace Engineering, University of Castilla-La Mancha, 13001 Toledo, Spain

Corresponding author: Zora Luburić (zora.luburic@hops.hr)

The research leading to these results has received funding from the European Union's Horizon 2020 research and innovation programme under grant agreement No 864298 (project ATTEST). The sole responsibility for the content of this document lies with the authors. It does not necessarily reflect the opinion of the Innovation and Networks Executive Agency (INEA) or the European Commission (EC). INEA or the EC are not responsible for any use that may be made of the information contained therein.

ABSTRACT Flexibility has become a requirement for modern power systems dominated by renewable generation sources. It can be extracted from different assets, ranging from demand response to fast generating units. This paper proposes an investment model that finds an optimal mix of transmission-level non-generation flexible assets: battery energy storage (BES), thyristor-controlled series compensators (TCSC), and transmission lines. The role of BES is to offset renewable generation in time, but its power converter is additionally utilized to provide voltage regulation by injecting/withdrawing reactive power. TCSC is used to alter power flows and increase existing lines' capacity, while new power lines are used to increase bulk power transfer. The proposed planning model uses a linearized AC OPF and employs Benders' decomposition to develop an iterative procedure for obtaining the optimal solution. The presented case study illustrates usefulness of the model for different BES costs and investment policies.

INDEX TERMS Battery energy storage, Benders' decomposition, FACTS devices, TCSC, transmission planning.

NOMENCLATURE

A. SETS

Ω^D	Set of representative days indexed with d
Ω^G	Set of piecewise blocks indexed with g
Ω^I	Set of thermal generators indexed with i
Ω^L	Set of lines consisting of existing lines, existing lines with TCSC and new lines $\Omega^L = \Omega^{L^{\mathrm{EX}}} \cup \Omega^{L^{\mathrm{TCSC}}} \cup \Omega^{L^{\mathrm{NEW}}}$ and indexed with l
Ω^N	Set of network buses indexed with n
Ω^R	Set of R-sided convex polygon slices indexed with r
Ω^S	Set of BES units indexed with s
Ω^T	Set of time periods indexed with t
Ω^W	Set of wind farms indexed with w
Ω^Z	Set of TCSC compensation blocks indexed with z

The associate editor coordinating the review of this manuscript and approving it for publication was S. Ali Arefifar.

B. VARIABLES

$ch_s^{\max}$	Rated power of converter of BES unit s (MVA)
$p_{d,t,s}^{\mathrm{ch/dis}}$	Active (dis)charging power of BES s in period t on day d (MW)
$p_{d,t,l}^{\mathrm{nm/mn}}$	Active power flow through line l from bus $n(m)$ to bus $m(n)$ in period t on day d (MW)
$\Delta p_{d,t,l}^{\mathrm{TCSC,\,max}}$	Active power flow through line l with TCSC in period t on day d (MW)
$pg_{d,t,i}$	Active power output of thermal generator i in period t on day d (MW)
$pls_{d,t,l}$	Active power losses on line l in period t on day d (MW)
$pw_{d,t,w}$	Active power output of wind farm w in period t on day d (MW)
$q_{d,t,s}^{\mathrm{ch/dis}}$	Reactive (dis)charging power of BES s in period t on day d (Mvar)

$q^{nm/mn}_{d,t,l}$ Reactive power flow through line l from bus $n(m)$ to bus $m(n)$ in period t in day d (Mvar)
$\Delta q^{TCSC,\,max}_{d,t,l}$ Reactive power flow through line l with TCSC in period t on day d (Mvar)
$qg_{d,t,i}$ Reactive power output of thermal generator i in period t on day d (Mvar)
$qls_{d,t,l}$ Reactive power losses on line l in period t on day d (Mvar)
$soc_{d,t,s}$ State of charge of BES s in period t on day d (MWh)
soc^{max}_{s} Installed capacity of BES s (MWh)
$v_{d,t,n}$ Voltage magnitude at bus n in period t on day d (kV)
$ws_{t,w}$ Wind spillage at farm w in period t on day d (MW)
$\theta_{d,t,n}$ Voltage angle at bus n in period t on day d (rad)
$\theta^{+}_{d,t,l}, \theta^{-}_{d,t,l}$ Slack variables on + and – voltage angle difference across line l in period t on day d (rad)
$\Delta v_{d,t,n}$ Voltage deviation at bus n in period t on day d
$\Delta\theta_{d,t,l,g}$ Size of gth linear block of angle difference across line l in period t on day d
$\xi^{BESpow(\upsilon)}_{d,s}$ Dual variable of constraint on variable ch^{max}_{s}
$\xi^{BESsoc}_{d,s}$ Dual variable of constraint on variable soc^{max}_{s}
$\xi^{TCSC}_{d,l}$ Dual variable of constraint on variable $\kappa^{TCSC}_{l,z}$
$\xi^{LINES}_{d,l}$ Dual variable of the constraint on variable v_l
v_l Binary variable equal to 1 if line l is built
$\kappa^{TCSC}_{l,z}$ Binary variable equal to 1 if TCSC capacity block z is selected
$p_{d,t,l}$ Variable equal to max $\left\{p^{nm}_{d,t,l}, p^{mn}_{d,t,l}\right\}$
$q_{d,t,l}$ Variable equal to max $\left\{q^{nm}_{d,t,l}, q^{mn}_{d,t,l}\right\}$

PARAMETERS

B_l Series susceptance of line l (S)
B^{sh}_{l} Shunt susceptance of line l (S)
$B^{TCSC}_{l,z}$ Series susceptance of line l with TCSC (S)
C^{BESen}_{s} Battery investment cost of BES unit s ($/MWh)
C^{BESpow}_{s} Converter investment cost of BES unit s ($/MVA)
$C^{TCSC}_{l,z}$ Investment cost of TCSC block z on line l ($)
C^{line}_{l} Investment cost of new lines l ($)
G_l Series conductance of transmission line l (S)
$G^{TCSC}_{l,z}$ Series conductance of line l with TCSC (S)
K_g Slope of the gth piecewise linear block
$\ell_{d,t,l}$ Takes value 1 if $\theta^{(\upsilon)}_{d,t,l} \geq 0$ on line l in period t on day d, and 0 otherwise
M Big enough constant
O^{gen}_{i} Production cost of thermal generator i ($/MW)
O^{wind}_{w} Production cost of wind farm w ($/MW)
$PD_{d,t,n}$ Active power demand at bus n in period t on day d (MW)
Pg^{max}_{i} Maximum active power output of generator i (MW)
$Pw^{det}_{d,t,w}$ Available power at wind farm w in period t on day d (MW)
$QD_{d,t,n}$ Reactive power demand at bus n in period t on day d (Mvar)
$Qg^{max}_{t,i}, Qg^{min}_{t,i}$ Maximum and minimum reactive power output of thermal generator i (Mvar)
RD_i Maximum ramp-down of thermal generator i (MW/h)
RU_i Maximum ramp-up of thermal generator i (MW/h)
S^{max}_{l} Power rating of line l (MVA)
Sg^{max}_{i} Maximum apparent power output of generator i (MVA)
X_l Reactance of line l (Ω)
θ^{max} Maximum allowed voltage angle (rad)
χ_d Number of days in a year represented by day d
$\sigma^{TCSC}_{l,z}$ Compensation level z of TCSC on line l
ΔV^{max}_{n} Maximum voltage magnitude deviation at bus n

I. INTRODUCTION

A. BACKGROUND AND MOTIVATION

One of major system-wide challenges in integrating renewable energy sources (RES) is their intermittent nature. This is a major change as compared to traditional, robust power systems characterized by steady, foreseeable and controllable generation [1]. Therefore, there is no doubt that new flexible assets need to be introduced and take a role in preserving the balance of generation and consumption [2]. Assuming that future generation will be based (almost) exclusively on RES, the system operator needs to ensure flexible assets at the transmission level as well to maximize utilization of non-controllable RES generation assets. Traditionally, the system operator may invest in new transmission lines to reduce congestion and improve utilization of RES generation, i.e. minimize its curtailment. However, line construction is very time-consuming and the investments are bulky making them economically inefficient. This inefficiency is especially apparent when utilization of the existing generation resources would be much more effective if parameters of specific lines are only slightly changed, which

can be accomplished using specific devices based on power electronics. Thyristor-controlled series capacitors (TCSC) comprise controlled reactors in parallel with sections of a capacitor bank. They change overall reactance of the line, thus affecting the power flows in the surrounding network. Installation of such devices can thus affect power flows and increase the utilization of RES generation in congested parts of the grid [3]. The third tool at the disposal to the system operator is battery energy storage (BES), which enables shifting energy in time, from periods of RES overproduction to periods of insufficient RES output. Although there are various applications of BES [4], and most of them are merchant oriented, in this paper we focus on the applications that improve social welfare and grid variables. Bidirectional AC/DC converters used to connect batteries to the AC grid inherently contain inductors and capacitors that can be utilized to inject/withdraw reactive power to/from the grid and control local voltage levels. This reactive power manipulation does not affect the battery state of charge, but reduces the available battery charging and discharging power.

To realistically model the power system operation and incorporate the effects of TCSC and BES on reactive power flows and voltage levels, this paper uses a linearized AC OPF (optimal power flow) model in which network losses and voltage magnitudes are variables. Since AC OPF is a nonlinear and nonconvex problem, linearization techniques are used to obtain the proposed network planning model looking at a target year. It simulates operation over a number of representative days that meticulously portray the entire year. Due to complexity of the proposed transmission expansion planning (TEP) problem, the iterative Benders' decomposition [5] is used to decompose it into a mixed-integer linear program (MILP) that serves as the investment master problem, and to several linear problems (LP), one for each representative day, that represent the operational sub-problems.

B. LITERATURE REVIEW

TEP models have had an important position in scientific literature for a long time. Since they consider the future power system topology and operating conditions, they often include uncertainty. For instance, in [6] the authors present a transmission network expansion planning problem considering uncertainty in demand. Due to a high complexity of such models, TEP problems either rely on heuristic methods, e.g. [7], or decomposition techniques, e.g. [8]. Furthermore, in order to preserve computational tractability of the model, power flows in these paper are represented by the DC model, which ignores voltage levels, losses and reactive power flows.

TEP problems have recently started considering BES assets, on top of transmission lines. This introduced a new dimension to TEP because BES move electricity in time, which complements transmission lines that move electricity in space. Therefore, BES does not entirely substitute transmission lines, but complements them depending on the power system characteristics, as shown in [9]. A mixed-integer model that considers only BES expansion in transmission systems is proposed in [10]. The model is solved in three stages, where the first stage determines optimal location of the BES, the second stage sets optimal BES size at each location, and the final stage determines actual operating costs used to calculate the economic viability of the installation. A stochastic multistage TEP model that considers both BES and transmission lines is presented in [11]. It utilizes BES both as a long-term solution and to defer investments in transmission lines under different renewable generation and load increase scenarios. A trilevel model where the upper-level problem optimizes the system operator's transmission line and BES investments, the middle-level determines the merchant energy storage investment decisions, and the lower-level simulates the market clearing process for representative days is formulated in [12]. The paper concludes that, even at low cost of BES, the system operator will give advantage to transmission lines since they are more lasting than BES. Also, increase in social welfare is mainly driven by the system operator's investments in transmission lines.

Another option to reduce bulky investments in new transmission lines, but still somewhat affect power flows and increase bandwidth of the transmission network, is to equip some of the existing lines with series compensation, as demonstrated in [13]. Fixed series compensation is especially suitable for networks with only slight congestion, often a result of the RES integration. To reduce RES curtailment, the model proposed in [14] minimizes investment costs in new lines, TCSC and reactive power sources. The model uses the linearized AC OPF formulation to assess reactive power flows, network losses, and voltage magnitudes. TCSC devices are modeled using binary variables. Each binary variable defines the level of installed compensation capacity at a specific line. In [15], optimal allocation of TCSC devices in an AC OPF model is proposed using a generalized Benders' decomposition approach. The proposed model is a two-stage stochastic program, where the first stage determines optimal locations and upper limits on TCSC devices. The second stage checks the AC feasibility of the obtained solution based on nonlinear programming (NLP). The results show that the number of allowed TCSC devices and computation time are not in direct correlation. Also, changing the maximum compensation level and the operating voltage range significantly affects the transmission lines selected for compensation. The authors in [16] find optimal location and size of TCSC devices to minimize the generation costs. An adaptive parallel seeker optimization algorithm is employed to solve a multi-objective OPF problem while a linear recursive sequence tool is utilized to reduce the search space.

C. CONTRIBUTION

With respect to the literature review above, this paper proposes an optimisation methodology for incorporating BES, series compensation (TCSC) and traditional reinforcement into transmission planning practice. Besides the model itself, we introduce two novelties to the literature. First, we model dynamic operation of TCSC in a mixed-integer linear fashion

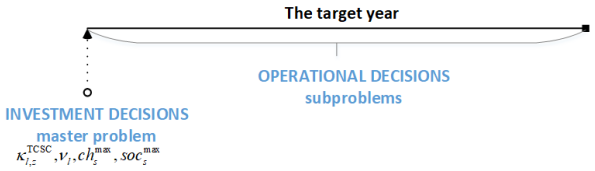

FIGURE 1. The relationship between the investment and the operation stages.

(the one in [15] is nonlinear). Dynamic TCSC operation means that compensation value of TCSC is actively adjusted at each operating time period between zero and the installed compensation capacity. Second, we use BES not only to inject or withdraw active power by discharging or charging the battery, which is customarily in the literature, but its AC/DC converter is also used to inject or withdraw reactive power, thus affecting network voltages. This adds another stream of value to the BES installation that has so far been ignored in the literature.

II. METHODOLOGY

Since computational tractability of a TEP problem using the linearized AC OPF is inadequate, we employ Benders' decomposition to dissolve the problem into two parts: i) Master problem – determines optimal investments in BES, TCSC and lines, and ii) Subproblem – solves the operational problem. The investment decisions from the master problem are then fixed in the subproblems to calculate the operating costs on representative days, as shown in Fig 1. In case the optimal solution is not achieved, the subproblems' sensitivities are used to construct the Benders' cut and the updated master problem is solved. Since the considered battery storage is a short-term storage (matter of hours), there is no need for coupling between the days, as in the case of long-term storage [17].

A. MASTER PROBLEM

Master problem is formulated as follows:

$$\begin{aligned}\underset{\aleph^{\mathrm{MP}}}{\text{Minimize}}\ E^{\mathrm{down}(\upsilon)} &= \sum_{l\in\Omega^{L^{\mathrm{NEW}}}} C_l^{\mathrm{line}}\cdot \nu_l^{(\upsilon)} \\ &+ \sum_{s\in\Omega^S}\left(C_s^{\mathrm{BESpow}}\cdot ch_s^{\max(\upsilon)} + C_s^{\mathrm{BESen}}\cdot soc_s^{\max(\upsilon)}\right) \\ &+ \sum_{l\in\Omega^{L^{\mathrm{TCSC}}}}\sum_{z\in\Omega^Z} C^{\mathrm{TCSC}}\cdot\kappa_{l,z}^{\mathrm{TCSC}(\upsilon)}\cdot\sigma_{l,z}^{\mathrm{TCSC}}(\upsilon)\cdot X_l \\ &+\alpha^{(\upsilon)} \qquad (1)\end{aligned}$$

$$\begin{aligned}\text{subject to: } \alpha^{(\upsilon)} &\geq \sum_{d\in\Omega^D} E_d^{\mathrm{SP}(k)} + \sum_{d\in\Omega^D}\sum_{l\in\Omega^{L^{\mathrm{NEW}}}} \xi_{d,l}^{\mathrm{LINE}(k)} \\ &\cdot\left(\nu_l^{(\upsilon)} - \nu_l^{(k)}\right) \\ &+ \sum_{d\in\Omega^D}\sum_{l\in\Omega^{L^{\mathrm{TCSC}}}}\sum_{z\in\Omega^Z} \xi_{d,l}^{\mathrm{TCSC}(k)} \\ &\cdot\left(\kappa_{l,z}^{\mathrm{TCSC}(\upsilon)} - \kappa_{l,z}^{\mathrm{TCSC}(k)}\right) \\ &+ \sum_{d\in\Omega^D}\sum_{s\in\Omega^S} \xi_{d,s}^{\mathrm{BESpow}(k)}\cdot\left(ch_s^{\max(\upsilon)} - ch_s^{\max(k)}\right) \\ &+ \xi_{d,s}^{\mathrm{BESsoc}(k)}\cdot\left(soc_s^{\max(\upsilon)} - soc_s^{\max(k)}\right) \\ &\forall k = 1,\ldots,\upsilon-1 \qquad (2)\end{aligned}$$

$$\sum_{z\in\Omega^Z}\kappa_{l,z}^{\mathrm{TCSC}(\upsilon)} \leq 1 \quad \forall l\in\Omega^{L^{\mathrm{TCSC}}} \qquad (3)$$

$$\alpha^{(\upsilon)} \geq \alpha^{\mathrm{down}}$$

$$\aleph^{\mathrm{MP}} = \left\{\kappa_{l,z}^{\mathrm{TCSC}(\upsilon)}, \alpha^{(\upsilon)}, \nu_l^{(\upsilon)}, E^{\mathrm{down}(\upsilon)}, ch_s^{\max(\upsilon)}, soc_s^{\max(\upsilon)}\right\}. \qquad (4)$$

Master problem objective function (1) minimizes total investment cost in new lines (first row), BES (second row) and TCSC (third row). All the investment costs are levelized to annual values in order to make them comparable to overall annual operating costs obtained from the subproblems. In other words, investment in a new transmission asset will be chosen if and only if the levelized daily cost of this investment in the master problem is lower than the sum of the weighed savings it achieves in the subproblems. Line investments are decided based on binary variable $\nu_l^{(\upsilon)}$ (1 – built; 0 – not built in iteration υ). On the other hand, BES investment is decided by two variables, $ch_s^{\max(\upsilon)}$, which sets the power capacity of the AC/DC converter for both (dis)charging the battery and reactive power compensation, and $soc_s^{\max(\upsilon)}$, which defines energy capacity of the battery. TCSC investment is based on binary variable $\kappa_{l,z}^{\mathrm{TCSC}(\upsilon)}$, which decides the reactance block z within parameter $\sigma_{l,z}^{\mathrm{TCSC}(\upsilon)}$ to be installed. This sets the maximum reactance compensation level of the existing line l in the subproblems. Investment in multiple TCSC blocks for each line is prohibited in constraint (3). The final item $\alpha^{(\upsilon)}$ in the objective function, defined in constraint (2), presents the Benders' cuts that include the subproblems' constraint sensitivities. Their function is to approximate the levelized operational costs formulated in the subproblems. Constraint (4) imposes the lower bound on Benders' cuts generated in (2) for each iteration. Master problem is represented by a set of variables in $\aleph^{\mathrm{MP}}$ referring to Benders' iteration υ.

B. SUBPROBLEMS

The subproblems formulated in (5)–(57) represent the operational problems where the investment variables obtained in the master problem are fixed. Variables from the subproblem set $\aleph^{\mathrm{SP}}$ are determined for each Benders' iteration υ.

$$\begin{aligned}\underset{\aleph^{\mathrm{SP}}}{\text{Minimize}}\ E_d^{\mathrm{SP}(\upsilon)} &= \chi_d\cdot\sum_{t\in\Omega^T}\left(\sum_{i\in\Omega^I} pg_{d,t,i}^{(\upsilon)}\cdot O_i^{\mathrm{gen}}\right. \\ &\left. + \sum_{w\in\Omega^W} pw_{d,t,w}^{(\upsilon)}\cdot O_w^{wind}\right) \qquad (5)\end{aligned}$$

subject to:

1) POWER BALANCE CONSTRAINTS

$$\sum_{w\in M^n} pw_{d,t,w}^{(\upsilon)} + \sum_{i\in M^n} pg_{d,t,i}^{(\upsilon)} + \sum_{o(l)\in M^n} p_{d,t,l}^{\mathrm{nm}(\upsilon)} + \sum_{d(l)\in M^n} p_{d,t,l}^{\mathrm{mn}(\upsilon)} - 0.5\sum_{l\in M^n} pls_{d,t,l}^{(\upsilon)} + \sum_{s\in M^n} p_{d,t,s}^{\mathrm{dis}(\upsilon)} = PD_{d,t,n} + \sum_{s\in M^n} p_{d,t,s}^{\mathrm{ch}(\upsilon)} \quad \forall n\in\Omega^N, t\in\Omega^T, d\in\Omega^D \tag{6}$$

$$\sum_{i\in M^n} qg_{d,t,i}^{(\upsilon)} + \sum_{o(l)\in M^n} q_{d,t,l}^{\mathrm{nm}(\upsilon)} + \sum_{d(l)\in M^n} q_{d,t,l}^{\mathrm{mn}(\upsilon)} - 0.5\sum_{l\in M^n} qls_{d,t,l}^{(\upsilon)} + \sum_{s\in M^n} q_{d,t,s}^{\mathrm{dis}(\upsilon)} = QD_{d,t,n} + \sum_{s\in M^n} q_{d,t,s}^{\mathrm{ch}(\upsilon)} \quad \forall n\in\Omega^N,\ t\in\Omega^T,\ d\in\Omega^D \tag{7}$$

Objective function (5) of subproblem d minimizes operating costs of conventional generators and wind power plants. Active power balance at each bus n is assured by constraint (6), which includes production of wind and thermal power plants, outgoing (from bus n to bus m) and incoming (from bus m to bus n) power flows, half of the active power line losses, power (dis)charging from BES and active power load. Reactive power balance in (7) includes reactive power injection/absorption of conventional generators, outgoing and incoming reactive power flows and losses, reactive power (dis)charging from BES, and reactive power load. Reactive power from BES units is based on the converter topology capable of producing capacitive and inductive power.

2) POWER FLOW CONSTRAINTS

$$p_{d,t,l}^{\mathrm{nm}(\upsilon)} = G_l\cdot\left(\Delta v_{d,t,n}^{(\upsilon)} - \Delta v_{d,t,m}^{(\upsilon)}\right) + B_l\cdot\theta_{d,t,l}^{(\upsilon)} \times\forall\{n,m\}\in l\in\Omega^{L^{\mathrm{EX,\,NEW}}},\quad t\in\Omega^T,\quad d\in\Omega^D \tag{8}$$

$$p_{d,t,l}^{\mathrm{mn}(\upsilon)} = -G_l\cdot\left(\Delta v_{d,t,n}^{(\upsilon)} - \Delta v_{d,t,m}^{(\upsilon)}\right) - B_l\cdot\theta_{d,t,l}^{(\upsilon)} \times\forall\{m,n\}\in l\in\Omega^{L^{\mathrm{EX,\,NEW}}},\quad t\in\Omega^T,\quad d\in\Omega^D \tag{9}$$

$$q_{d,t,l}^{\mathrm{nm}(\upsilon)} = -B_l^{\mathrm{sh}}\cdot\left(1+2\Delta v_{d,t,n}^{(\upsilon)}\right) - G_l\cdot\theta_{d,t,l}^{(\upsilon)} + B_l\cdot\left(\Delta v_{d,t,n}^{(\upsilon)} - \Delta v_{d,t,m}^{(\upsilon)}\right) \times\forall\{n,m\}\in l\in\Omega^{L^{\mathrm{EX,\,NEW}}},\quad t\in\Omega^T,\quad d\in\Omega^D \tag{10}$$

$$q_{d,t,l}^{\mathrm{mn}(\upsilon)} = -B_l^{\mathrm{sh}}\cdot\left(1+2\Delta v_{d,t,m}^{(\upsilon)}\right) + G_l\cdot\theta_{d,t,l}^{(\upsilon)} - B_l\cdot\left(\Delta v_{d,t,n}^{(\upsilon)} - \Delta v_{d,t,m}^{(\upsilon)}\right) \times\forall\{m,n\}\in l\in\Omega^{L^{\mathrm{EX,\,NEW}}},\quad t\in\Omega^T,\quad d\in\Omega^D \tag{11}$$

$$\left(\nu_l^{(\upsilon)}-1\right)\cdot M \le p_{d,t,l}^{\mathrm{nm}(\upsilon)} - \Delta p_{d,t,l}^{(\upsilon)} \le \left(1-\nu_l^{(\upsilon)}\right)\cdot M \times\forall\{n,m\}\in l\in\Omega^{L^{\mathrm{NEW}}},\quad t\in\Omega^T,\quad d\in\Omega^D \tag{12}$$

$$\left(\nu_l^{(\upsilon)}-1\right)\cdot M \le p_{d,t,l}^{\mathrm{mn}(\upsilon)} - \Delta p_{d,t,l}^{(\upsilon)} \le \left(1-\nu_l^{(\upsilon)}\right)\cdot M \times\forall\{m,n\}\in l\in\Omega^{L^{\mathrm{NEW}}},\quad t\in\Omega^T,\quad d\in\Omega^D \tag{13}$$

$$\left(\nu_l^{(\upsilon)}-1\right)\cdot M \le q_{d,t,l}^{\mathrm{nm}(\upsilon)} - \Delta q_{d,t,l}^{(\upsilon)} \le \left(1-\nu_l^{(\upsilon)}\right)\cdot M \times\forall\{n,m\}\in l\in\Omega^{L^{\mathrm{NEW}}},\quad t\in\Omega^T,\quad d\in\Omega^D \tag{14}$$

$$\left(\nu_l^{(\upsilon)}-1\right)\cdot M \le q_{d,t,l}^{\mathrm{mn}(\upsilon)} - \Delta q_{d,t,l}^{(\upsilon)} \le \left(1-\nu_l^{(\upsilon)}\right)\cdot M \times\forall\{m,n\}\in l\in\Omega^{L^{\mathrm{NEW}}},\quad t\in\Omega^T,\quad d\in\Omega^D \tag{15}$$

Active and reactive power flow constraints for both the existing and new lines are imposed through eqs. (8)–(11). The formulation calculates their values for each direction as explained in [18]. Constraints (12)–(15) are used to force active and reactive power flows through newly constructed lines (these are candidate lines whose binary variable ν_l is equal to 1) to $\Delta p_{d,t,l}^{(\upsilon)}$ and $\Delta q_{d,t,l}^{(\upsilon)}$, which are defined as the right-hand sides of (8) and (10). The *big M* method is used to avoid nonlinearity due to binary variable determining if a line is built or not.

Maximum and minimum bounds on power flows on lines equipped with TCSC are set as follows:

$$\Delta p_{d,t,l,z}^{\mathrm{TCSC,max}(\upsilon)} = G_{l,z}^{\mathrm{TCSC}}\cdot\left(\Delta v_{d,t,n}^{(\upsilon)} - \Delta v_{d,t,m}^{(\upsilon)}\right) + B_{l,z}^{\mathrm{TCSC}}\cdot\theta_{d,t,l}^{(\upsilon)} \times\forall z\in\Omega^Z,\quad \{n,m\}\in l\in\Omega^{L^{\mathrm{TCSC}}},\quad t\in\Omega^T,\quad d\in\Omega^D \tag{16}$$

$$\Delta q_{d,t,l,z}^{\mathrm{TCSC,max}(\upsilon)} = -B_l^{\mathrm{sh}}\cdot\left(1+2\Delta v_{d,t,n}^{(\upsilon)}\right) + B_{l,z}^{\mathrm{TCSC}}\cdot\left(\Delta v_{d,t,n}^{(\upsilon)} - \Delta v_{d,t,m}^{(\upsilon)}\right) - G_{l,z}^{\mathrm{TCSC}((\upsilon)\cdot\theta_{d,t,l}^{(\upsilon)}} \times\forall z\in\Omega^Z,\quad \{n,m\}\in l\in\Omega^{L^{\mathrm{TCSC}}},\quad t\in\Omega^T,\quad d\in\Omega^D \tag{17}$$

$$\Delta p_{d,t,l,z}^{\mathrm{TCSC,min}(\upsilon)} := \Delta p_{d,t,l}^{(\upsilon)} \tag{18}$$

$$\Delta q_{d,t,l,z}^{\mathrm{TCSC,min}(\upsilon)} := \Delta q_{d,t,l}^{(\upsilon)} \tag{19}$$

$$G_{l,z}^{\mathrm{TCSC}} = \frac{R_l}{(R_l)^2 + \left(X_l\cdot\left(1-\sigma_{l,z}^{\mathrm{TCSC}}\right)\right)^2} \times\forall z\in\Omega^Z,\quad \{n,m\}\in l\in\Omega^{L^{\mathrm{TCSC}}} \tag{20}$$

$$B_{l,z}^{\mathrm{TCSC}} = \frac{X_l \cdot \left(1 - \sigma_{l,z}^{\mathrm{TCSC}}\right)}{(R_l)^2 + \left(X_l \cdot \left(1 - \sigma_{l,z}^{\mathrm{TCSC}}\right)\right)^2} \times \forall z \in \Omega^Z, \quad \{n,m\} \in l \in \Omega^{L^{\mathrm{TCSC}}} \tag{21}$$

Eqs. (16) and (17) calculate maximum active and reactive power flows using susceptance and conductance values of the installed TCSC capacity block determined in (20)–(21), as further explained in [14]. Eqs. (18)–(19) set the minimum power flows to the values without TCSC. Thus, power flows through a line with TCSC can be increased up to the level determined by the installed TCSC capacity.

Active power flows through lines equipped with TCSC are calculated as follows:

$$\kappa_{l,f}^{\mathrm{TCSC}(\upsilon)} \cdot M - \sum_{z \in \Omega^Z | z \neq f} \kappa_{l,z}^{\mathrm{TCSC}(\upsilon)} \cdot M + \ell_{d,t,l} \cdot \Delta p_{d,t,l,f}^{\mathrm{TCSC,min}(\upsilon)} - (1 - \ell_{d,t,l}) \cdot M - M \leq p_{d,t,l,f}^{(\upsilon)} \times \forall f \in \{1, \ldots, Z\}, l \in \Omega^{L^{\mathrm{TCSC}}}, \quad t \in \Omega^T, \ d \in \Omega^D \tag{22}$$

$$-\kappa_{l,f}^{\mathrm{TCSC}(\upsilon)} \cdot M + \sum_{z \in \Omega^Z | z \neq f} \kappa_{l,z}^{\mathrm{TCSC}(\upsilon)} \cdot M + \ell_{d,t,l} \cdot \Delta p_{d,t,l,f}^{\mathrm{TCSC,max}(\upsilon)} + (1 - \ell_{d,t,l}) \cdot M + M \geq p_{d,t,l,f}^{(\upsilon)} \times \forall f \in \{1, \ldots, Z\}, \quad l \in \Omega^{L^{\mathrm{TCSC}}}, \ t \in \Omega^T, \ d \in \Omega^D \tag{23}$$

$$\kappa_{l,f}^{\mathrm{TCSC}(\upsilon)} \cdot M - \sum_{z \in \Omega^Z | z \neq f} \kappa_{l,z}^{\mathrm{TCSC}(\upsilon)} \cdot M - (1 - \ell_{d,t,l}) \cdot \Delta p_{d,t,l,f}^{\mathrm{TCSC,max}(\upsilon)} - \ell_{d,t,l} \cdot M - M \leq p_{d,t,l,f}^{(\upsilon)} \times \forall f \in \{1, \ldots, Z\}, \quad l \in \Omega^{L^{\mathrm{TCSC}}}, \ t \in \Omega^T, \ d \in \Omega^D \tag{24}$$

$$-\kappa_{l,f}^{\mathrm{TCSC}(\upsilon)} \cdot M + \sum_{z \in \Omega^Z | z \neq f} \kappa_{l,z}^{\mathrm{TCSC}(\upsilon)} \cdot M - (1 - \ell_{d,t,l}) \cdot \Delta p_{d,t,l,f}^{\mathrm{TCSC,min}(\upsilon)} + \ell_{d,t,l} \cdot M + M \geq p_{d,t,l}^{(\upsilon)} \times \forall f \in \{1, \ldots, Z\}, \quad l \in \Omega^{L^{\mathrm{TCSC}}}, \ t \in \Omega^T, \ d \in \Omega^D \tag{25}$$

Set of constraints (22)–(25) determines power flows on lines with installed TCSC based on decision variable $\kappa_{l,f}^{\mathrm{TCSC}}$ from the master problem. Parameter $\ell_{d,t,l}$ takes value 1 if $\theta_{d,t,l}^{(\upsilon)} \geq 0$ and 0 otherwise. It is used to define the actual direction of the line flow and is determined before solving the TEP problem. Further information on the role of this parameter is available in [19]. Dynamic change of TCSC reactance adjusts line flow to optimal value within the given range of the installed compensation level at each time period. Fig. 2 visualizes how (22)–(25) work. Eq. (22) sets the lower bound to the power flow without TCSC, while (23) sets the power flow upper bound, i.e. the maximum possible power flow with TCSC installed. Negative power flow direction is bounded by (24) and (25). Eqs. (22)–(25) have their corresponding counterparts for reactive power where letter p is replaced by letter q.

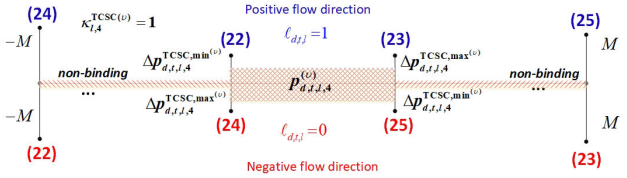

FIGURE 2. The explanations of TCSC constraints (22)–(25) on active power flow (e.g. if the compensation level 4 is installed).

Power flow limits on newly installed power lines are imposed using binary variable ν_l:

$$-\nu_l^{(\upsilon)} \cdot S_l^{\max} \leq p_{d,t,l}^{(\upsilon)} \leq \nu_l^{(\upsilon)} \cdot S_l^{\max} \times \forall l \in \Omega^{L^{\mathrm{NEW}}}, \quad t \in \Omega^T, \ d \in \Omega^D \tag{26}$$

$$-\nu_l^{(\upsilon)} \cdot S_l^{\max} \leq q_{d,t,l}^{(\upsilon)} \leq \nu_l^{(\upsilon)} \cdot S_l^{\max} \times \forall l \in \Omega^{L^{\mathrm{NEW}}}, \quad t \in \Omega^T, \ d \in \Omega^D \tag{27}$$

The second-order cone constraint on maximum active and reactive power flows are limited by constraint (28). To avoid nonlinearity, the feasible region is described as an R-sided convex regular polygon [20].

$$\left(p_{d,t,l}^{(\upsilon)}\right)^2 + \left(q_{d,t,l}^{(\upsilon)}\right)^2 \leq \left(S_l^{\max}\right)^2 \quad \forall l \in \Omega^L, \ t \in \Omega^T, \ d \in \Omega^D \tag{28}$$

Constraint on voltage magnitude is defined as:

$$0 \leq \Delta v_{d,t,n}^{(\upsilon)} \leq \Delta V_n^{\max} \quad \forall n \in \Omega^N, \ t \in \Omega^T, \ d \in \Omega^D \tag{29}$$

Constraints representing piecewise-linearized losses are:

$$\theta_{d,t,l}^{(\upsilon)} = \theta_{d,t,l}^{+(\upsilon)} - \theta_{d,t,l}^{-(\upsilon)} \quad \forall l \in \Omega^L, \ t \in \Omega^T, \ d \in \Omega^D \tag{30}$$

$$\sum_{g \in \Omega^G} \Delta\theta_{d,t,l,g}^{(\upsilon)} = \theta_{d,t,l}^{+(\upsilon)} + \theta_{d,t,l}^{-(\upsilon)} \quad \forall g \in \Omega^G, \ l \in \Omega^L, \ t \in \Omega^T, \quad d \in \Omega^D \tag{31}$$

$$0 \leq \Delta\theta_{d,t,l,g}^{(\upsilon)} \leq \frac{\theta^{\max}}{G} \quad \forall g \in \Omega^G, \ l \in \Omega^L, \ t \in \Omega^T, \ d \in \Omega^D \tag{32}$$

$$\Delta\theta_{d,t,l,g}^{(\upsilon)} \leq \Delta\theta_{d,t,l,g-1}^{(\upsilon)} \quad \forall g \in \Omega^G, \ l \in \Omega^L, \ t \in \Omega^T, \quad d \in \Omega^D \tag{33}$$

$$0 \leq \Delta\theta_{d,t,l,g}^{(\upsilon)} \leq \frac{\theta^{\max}}{G} + \frac{\left[\left(1 - \nu_l^{(\upsilon)}\right) \cdot \pi\right]}{G} \times \forall g \in \Omega^G, \quad l \in \Omega^{L^{\mathrm{NEW}}}, \ t \in \Omega^T, \ d \in \Omega^D \tag{34}$$

$$pls_{d,t,l}^{(\upsilon)} = G_l \cdot \sum_{g \in \Omega^G} K_g \cdot \Delta\theta_{d,t,l,g}^{(\upsilon)} \times \forall g \in \Omega^G, \quad l \in \Omega^L, \ t \in \Omega^T, d \in \Omega^D \tag{35}$$

$$0 \le pls_{d,t,l}^{(\upsilon)} \le v_l^{(\upsilon)} \cdot G_l \cdot \left(\theta^{\max}\right)^2 \quad \forall l \in \Omega^{L^{\text{NEW}}}, \; t \in \Omega^T, \quad d \in \Omega^D \tag{36}$$

$$0 \le -pls_{d,t,l}^{(\upsilon)} + G_l \cdot \sum_{g \in \Omega^G} K_g \cdot \Delta\theta_{d,t,l,g}^{(\upsilon)} \le \left(1 - v_l^{(\upsilon)}\right) \cdot M \quad \forall l \in \Omega^{L^{\text{NEW}}}, \; t \in \Omega^T, \; d \in \Omega^D \tag{37}$$

$$qls_{d,t,l}^{(\upsilon)} = -B_l \cdot \sum_{g \in \Omega^G} K_g \cdot \Delta\theta_{d,t,l,g}^{(\upsilon)} \times \forall g \in \Omega^G, \quad l \in \Omega^L, \; t \in \Omega^T, \; d \in \Omega^D \tag{38}$$

$$0 \le qls_{d,t,l}^{(\upsilon)} \le v_l^{(\upsilon)} \cdot B_l \cdot \left(\theta^{\max}\right)^2 \quad \forall l \in \Omega^{L^{\text{NEW}}}, \; t \in \Omega^T, d \in \Omega^D \tag{39}$$

$$0 \le -qls_{d,t,l}^{(\upsilon)} - B_l \cdot \sum_{g \in \Omega^G} K_g \cdot \Delta\theta_{d,t,l,g}^{(\upsilon)} \le \left(1 - v_l^{(\upsilon)}\right) \cdot M \quad \forall g \in \Omega^G, \; l \in \Omega^{L^{\text{NEW}}}, \; t \in \Omega^T, \quad d \in \Omega^D \tag{40}$$

$$K_g = (2g - 1) \cdot \frac{\theta^{\max}}{G} \quad \forall g \in \Omega^G \tag{41}$$

Active and reactive power losses in (30)–(41) are denoted with $pls_{d,t,l} \approx G_l \cdot \theta_{d,t,l}^2$ and $qls_{d,t,l} \approx -B_l \cdot \theta_{d,t,l}^2$ and modeled using piecewise linearization of the square of voltage angles [18]. Two slack variables in (30) are used to replace the absolute value of voltage angle $\theta_{d,t,l}^{(\upsilon)}$. Constraint (31) forces both positive and negative values to be calculated in the first quadrant. Constraint (32) limits variable $\Delta\theta_{d,t,l,g}$. Constraint (33) is used to avoid fictitious network losses, while (34) stands only for new lines. Active power losses are then calculated in (35), while (36)–(37) are binding only if new lines are built. Constraints (38)–(40) are reactive counterparts of constraints (35)–(37). Eq. (41) calculates slope K_g at each linearized block of the quadratic voltage magnitude.

3) GENERATION CONSTRAINTS

Constraints on the operation of conventional generation units:

$$0 \le pg_{d,t,i}^{(\upsilon)} \le Pg_i^{\max} \quad \forall i \in \Omega^I, \; t \in \Omega^T, \; d \in \Omega^D \tag{42}$$

$$pg_{d,t,i}^{(\upsilon)} - pg_{d,t-1,i}^{(\upsilon)} \le RU_i \quad \forall i \in \Omega^I, \; t \in \Omega^T, \; \forall d \in \Omega^D \tag{43}$$

$$pg_{d,t,i}^{(\upsilon)} - pg_{d,t-1,i}^{(\upsilon)} \ge -RD_i \quad \forall i \in \Omega^I, \; t \in \Omega^T, \; d \in \Omega^D \tag{44}$$

$$Qg_{d,t,i}^{\min} \le qg_{d,t,i}^{(\upsilon)} \le Qg_{d,t,i}^{\max} \quad \forall i \in \Omega^I, \; t \in \Omega^T, \; d \in \Omega^D \tag{45}$$

$$\left(pg_{d,t,i}^{(\upsilon)}\right)^2 + \left(qg_{d,t,i}^{(\upsilon)}\right)^2 \le \left(Sg_i^{\max}\right)^2 \quad \forall i \in \Omega^I, \; t \in \Omega^T, \; d \in \Omega^D \tag{46}$$

Maximum active power production limits of conventional generators are set in (42), while their up and down ramp limits are imposed in (43) and (44). Maximum and minimum reactive power output is limited in (45). Second-order cone constraint (46) represents the feasible operation area of generators, whose implementation is linearized as in [20].

Available wind power output is partitioned between utilized wind power and wind spillage:

$$pw_{d,t,w}^{(\upsilon)} + ws_{d,t,w}^{(\upsilon)} = Pw_{d,t,w}^{\text{det}} \quad \forall w \in \Omega^W, \; t \in \Omega^T, \; d \in \Omega^D \tag{47}$$

4) BATTERY ENERGY STORAGE CONSTRAINTS

$$0 \le p_{d,t,s}^{\text{ch}(\upsilon)} \le ch_s^{\max(\upsilon)} \quad \forall s \in \Omega^S, \; t \in \Omega^T, \; d \in \Omega^D \tag{48}$$

$$0 \le p_{d,t,s}^{\text{dis}(\upsilon)} \le ch_s^{\max(\upsilon)} \quad \forall s \in \Omega^S, \; t \in \Omega^T, \; d \in \Omega^D \tag{49}$$

$$0 \le q_{d,t,s}^{\text{ch}(\upsilon)} \le ch_s^{\max(\upsilon)} \quad \forall s \in \Omega^S, \; t \in \Omega^T, \; d \in \Omega^D \tag{50}$$

$$0 \le q_{d,t,s}^{\text{dis}(\upsilon)} \le ch_s^{\max(\upsilon)} \quad \forall s \in \Omega^S, \; t \in \Omega^T, \; 'd \in \Omega^D \tag{51}$$

$$\left(p_{d,t,s}^{\text{ch}(\upsilon)}\right)^2 + \left(q_{d,t,s}^{\text{ch}(\upsilon)}\right)^2 \le \left(ch_s^{\max(\upsilon)}\right)^2 \times \forall s \in \Omega^S, \quad t \in \Omega^T, \; d \in \Omega^D \tag{52}$$

$$\left(p_{d,t,s}^{\text{dis}(\upsilon)}\right)^2 + \left(q_{d,t,s}^{\text{dis}(\upsilon)}\right)^2 \le \left(ch_s^{\max(\upsilon)}\right)^2 \times \forall s \in \Omega^S, \quad t \in \Omega^T, \; d \in \Omega^D \tag{53}$$

$$0 \le soc_{d,t,s}^{(\upsilon)} \le soc_s^{\max(\upsilon)} \quad \forall s \in \Omega^S, \; t \in \Omega^T, \; d \in \Omega^D \tag{54}$$

$$soc_{d,t,s}^{(\upsilon)} = soc_{d,t-1,s}^{(\upsilon)} + p_{d,t,s}^{\text{ch}(\upsilon)} \cdot \eta^{\text{ch}} - \frac{p_{d,t,s}^{\text{dis}(\upsilon)}}{\eta^{\text{dis}}} \quad \forall s \in \Omega^S, \; t \in \Omega^T, \quad d \in \Omega^D \tag{55}$$

Constraints on active and reactive (dis)charging power of BES, i.e. rated power of its AC/DC converter, are set by (48)-(51). Quadratic constraints (52)-(53) describing the operation area of the converter are linearized in the same way as (28). The inverter can use its entire rating to supply reactive power, however, in that case the battery cannot be charged nor discharged. Battery state of charge is in (54) limited by the maximum state of charge determined in the master problem. State of charge in (55) is determined based on the amount of injected/absorbed active power during the discharging/charging.

5) INTERACTION WITH THE MASTER PROBLEM

Constraints on the decision variables from the master problem:

$$v_l^{(\upsilon)} = v_l^{\text{fixed}(\upsilon)} \; : \xi_{d,l}^{\text{LINES}(\upsilon)} \quad \forall l \in \Omega^{L^{\text{NEW}}}, \; d \in \Omega^D \tag{56}$$

$$\kappa_{l,z}^{\mathrm{TCSC}(\upsilon)} = \kappa_{l,z}^{\mathrm{TCSC,fixed}(\upsilon)} : \xi_{d,l}^{\mathrm{TCSC}(\upsilon)} \quad \forall l \in \Omega^{L^{\mathrm{TCSC}}}, \; d \in \Omega^{D} \tag{57}$$

$$soc_{s}^{\max(\upsilon)} = soc_{s}^{\max,\mathrm{fixed}(\upsilon)} : \xi_{d,s}^{\mathrm{soc}(\upsilon)} \quad \forall s \in \Omega^{S}, \; d \in \Omega^{D} \tag{58}$$

$$ch_{s}^{\max(\upsilon)} = ch_{s}^{\max,\mathrm{fixed}(\upsilon)} : \xi_{d,s}^{\mathrm{BESpow}(\upsilon)} \quad \forall s \in \Omega^{S}, \; d \in \Omega^{D} \tag{59}$$

$$\begin{aligned} E^{\mathrm{up}(\upsilon)} = & \sum_{d \in \Omega^{D}} E_{d}^{\mathrm{SP}(\upsilon)} + \sum_{l \in \Omega^{L^{\mathrm{NEW}}}} \nu_{l}^{\mathrm{fixed}} \cdot C_{l}^{\mathrm{line}} \\ & + \sum_{s \in \Omega^{S}} \left(C^{\mathrm{BESpow}} \cdot ch_{s}^{\max,\mathrm{fixed}} + C^{\mathrm{BESen}} \right. \\ & \left. \cdot soc_{s}^{\max,\mathrm{fixed}} \right) \\ & + \sum_{l \in \Omega^{L^{\mathrm{TCSC}}}} C^{\mathrm{TCSC}} \cdot \kappa_{l,z}^{\mathrm{TCSC,fixed}(\upsilon)} \cdot \sigma_{l,z}^{\mathrm{TCSC}} \cdot X_{l} \end{aligned} \tag{60}$$

Investment variables in (56)–(59) are fixed to the decisions derived in the master problem. The upper bound of the original problem is obtained in (60). The variables in the subproblem are:

$$\begin{aligned} \aleph^{\mathrm{SP}} = \Big\{ & pg_{d,t,i}^{(\upsilon)}, p_{d,t,l}^{(\upsilon)}, p_{d,t,l}^{\mathrm{nm}(\upsilon)}, p_{d,t,l}^{\mathrm{mn}(\upsilon)}, qg_{d,t,i}^{(\upsilon)}, q_{d,t,l}^{(\upsilon)}, p_{d,t,l}^{(\upsilon)}, \\ & q_{d,t,l}^{\mathrm{nm}(\upsilon)}, q_{d,t,l}^{\mathrm{mn}(\upsilon)}, \Delta v_{d,t,n}^{(\upsilon)}, \theta_{d,t,n}^{(\upsilon)}, \theta_{d,t,l}^{+(\upsilon)}, \theta_{d,t,l}^{-(\upsilon)}, pls_{d,t,l}^{(\upsilon)}, \\ & qls_{d,t,l}^{(\upsilon)}, \Delta\theta_{d,t,l,g}^{(\upsilon)}, pw_{d,t,w}^{(\upsilon)}, ws_{d,t,w}^{(\upsilon)}, soc_{d,t,s}^{(\upsilon)}, p_{d,t,s}^{\mathrm{ch}(\upsilon)}, \\ & p_{d,t,s,}^{\mathrm{dis}(\upsilon)}, \nu_{l}^{(\upsilon)}, \kappa_{l,z}^{\mathrm{TCSC}(\upsilon)}, ch_{s}^{\max(\upsilon)}, soc_{s}^{\max(\upsilon)} \Big\}. \end{aligned}$$

C. THE PROPOSED BENDERS' ALGORITHM

1) Initialization: Set $\upsilon = 1$, $E^{\mathrm{down}(\upsilon)} = -\infty$, and complicating decision variables: $\nu_{l}^{\mathrm{fixed}(\upsilon)} = 0$, $\kappa_{l,z}^{\mathrm{TCSC,fixed}(\upsilon)} = 0$, $soc_{s}^{\max,\mathrm{fixed}(\upsilon)} = 0$, $ch_{s}^{\max,\mathrm{fixed}(\upsilon)} = 0$.
2) Initial subproblem and time period: Consider day $d = 1$, time period $t = 1$.
3) Subproblems solution: Solve (5) − (59) for each day d and time period t and calculate $E^{\mathrm{up}(\upsilon)}$ as in (60).
4) Convergence check: If $\left| E^{\mathrm{up}(\upsilon)} - E^{\mathrm{down}(\upsilon)} \right| \leq \epsilon$, the optimal solution with level of accuracy ϵ has been obtained. Otherwise, calculate the sensitivities to build the Benders' cut. Then, set $\upsilon \leftarrow \upsilon + 1$.
5) Master problem solution: Solve (1) − (4), calculate $E^{\mathrm{down}(\upsilon)}$ and update the values of complicating decision variables. Then, continue to step 3.

III. CASE STUDY

A. INPUT DATA

The proposed model is applied to a modified IEEE 24-bus system with high installed wind power capacity. Detailed data on this power system can be found in [21]. The target year is modeled by a set of five representative days with hourly periods selected based on the scenario reduction algorithm described in [22]. It uses an iterative approach to select days that minimize the probability distance between the original set of 365 days and the reduced one. Each representative day has its assigned weight according to its occurrence frequency in the target year. Wind production and demand for five characteristic days are shown Fig. 3 and Fig. 4. As reported in [23] and confirmed in our own numerical experiments, five representative days are sufficient to ensure numerical stability of the solution.

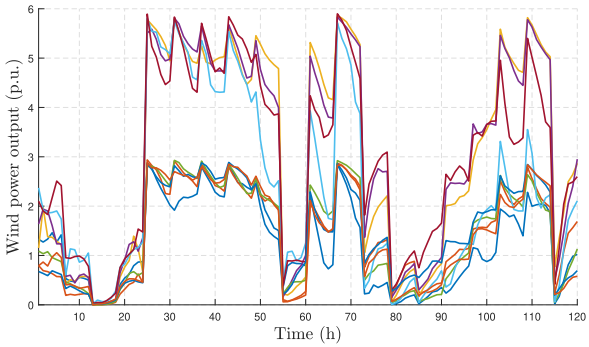

FIGURE 3. Wind production scenarios over five representative days.

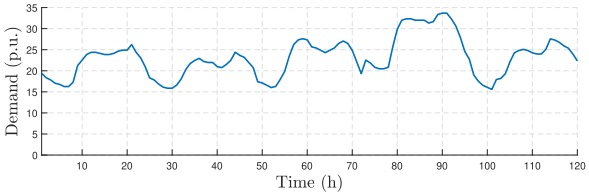

FIGURE 4. Demand profile over five representative days.

BES installation is allowed at three preselected buses: $s102$, $s114$, and $s120$. TCSC installation is enabled at lines connecting buses $s102$–$s104$ ($l4$) and $s115$–$s121$ ($l25$), both belonging to a group of long-distance lines. Maximum allowed TCSC compensation level is 0.6 [24]. Four discrete maximum compensation levels are allowed: 0.15, 0.3, 0.45, and 0.6. The third investment option are new power lines between buses $s101$–$s102$ ($l41$), $s116$–$s117$ ($l39$), $s116$–$s119$ ($l40$), and $s117$–$s118$ ($l42$). Preselection of the candidates for BES, TCSC and new lines highly reduces the feasible area and improves computational performance. In reality, such preselecation is based on operator's experience as well as geographical and legal constraints, especially when it comes to the construction of new lines.

Investment costs are calculated using capital recovery factor as in [12], with annual interest rate 5%, BES lifetime 15 years, TCSC lifetime 20 years, and lines lifetime 40 years. Since the investment is aimed for the target year, all investment costs are scaled to one year. We consider three distinct BES investment costs: \$17/kWh and \$425/kW (high), \$13/kWh and \$325/kW (medium), and \$10/kWh and \$250/kW (low). TCSC investment costs are based on the cost function from [25] and shown in Table 1. Line investments are based on data from [26], resulting in 153,120\$/year for $l39$, 138,040\$/year for $l40$, 32,712\$/year for $l41$, and 92,800\$/year for $l42$.

TABLE 1. Investment costs of TCSC devices ($/year).

TCSC lines	Compensation level (p.u.) 0.15	0.3	0.45	0.6
$l4$	64,569	129,139	193,709	258,278
$l25$	161,278	322,557	483,836	645,115

TABLE 2. Investment results.

Options	Line	BES (MWh/MVA)	TCSC	Costs (m$)	CPU (min)
high.all	$l41$	x	x	0.032	6.78
high.flex	-	x	$l4$(0.6)	0.258	8.95
medium.all	$l41$	$s120$(150;23.8)	x	0.811	14.59
medium.flex	-	$s120$(124;20.5)	$l4$(0.45)	0.864	27.36
low.all	$l41$	$s102$(150;27.7) $s114$(150;27.7) $s120$(150;27.7)	x	2.059	37.46
low.flex	-	$s114$(150;27.7) $s120$(150;27.7)	$l4$(0.6)	1.612	58.01

B. RESULTS

Optimal investments for three BES costs are shown in Table 2. Allowing investment in all three technologies (option *all*) results in investment in line $l41$ for all three BES costs. In case of the high BES cost, this is the only investment in the network. For medium cost of BES, the optimal investment plan also includes a 150 MWh/23.8 MW BES at bus $s120$. The low BES cost scenario results in even higher BES capacity divided across buses $s102$, $s114$ and $s120$. No investment in TCSC is observed in any of these cases. In order to further examine the behavior of the proposed model, we include *flex* option, which allows only installation of TCSC and BES. The high BES cost results in a TCSC installation on line $l4$. This investment, but with reduced capacity, exist for the medium BES cost as well, but is supplemented with BES investment at bus $s120$. The low BES cost scenario keeps the TCSC at bus $l4$ and installs 150 MWh/27.7 MW BES at buses $s114$ and $s120$.

The computation times reached by each option are provided in Table 2. The solution times range from 6.78 minutes for the *high.all* option to 58.01 minutes for *low.flex* option. The solution times increase as the prices of BES are lower due to multiple attractive options on siting and sizing of BES. Also, the optimizations with *all* options is in general completed quicker than for *flex* options as it considers more assets.

Fig. 5 shows the convergence rate of the Benders' algorithm for each option. The convergence is slower as BES starts to be more attractive option due to reduced price (low option). The spread on the number of iterations is quite wide, as option *high.all* requires only 17 iterations to reach the optimal solution, the option *low.flex* requires 119 iterations to reach the ϵ-criterion specified under subsection II-C.

Operation results are shown in Table 3. Generally, the savings are higher in *all* options cases (0.974% for the high BES cost) than for *flex* options cases (0.292% for the high BES cost). As the BES costs reduce, the increased investment in BES further reduce the system operating costs. Wind curtailment is also reduced with increased investments, reaching 6% for the *low.all* option. Reduction of losses is slightly higher when investment in new line is performed (option *high.all*) than for installation of TCSC (option *high.flex*). Network losses are generally reduced by 1-2% after the investments. The lowest reduction is achieved for option *low.all* (0.151%). This is caused by installation of BES at bus $s102$, which reduces wind curtailment at that bus, but increases losses on the surrounding lines. The increased losses are explained by increased flows in hours when the BES is discharged and this electricity, along with electricity produced by inexpensive generators at bus $s102$, is transferred to the northern part of the grid with high loads.

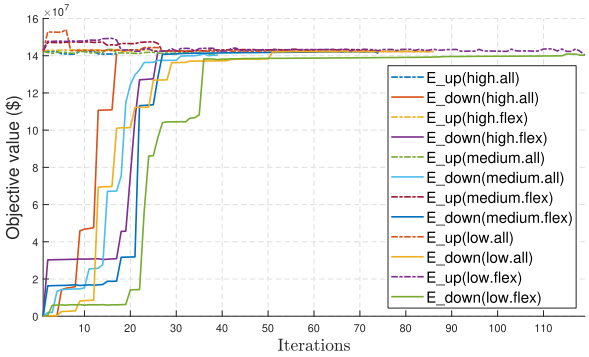

FIGURE 5. Number of iterations to obtain optimal solution.

TABLE 3. Operating costs, wind curtailment and energy losses.

Options	Total costs ($)	Wind curtailment (MWh)	Losses (MWh)
no investment	142,416,862	1,279,322	357,750
high.all	-0.974%	-0.189%	-1.692%
high.flex	-0.292%	-0.175%	-1.500%
medium.all	-1.528%	-2.062%	-1.891%
medium.flex	-0.685%	-1.963%	-0.811%
low.all	-2.664%	-5.976%	-0.151%
low.flex	-1.497%	-4.422%	-1.121%

Installation of TCSC helps power line loadability, as shown in Fig. 6. Higher TCSC compensation levels significantly increases utilization of line $l4$. The red line corresponds to line loading in *high.flex* option (compensation level 0.6), while the blue line shows load levels for *medium.flex* option (compensation level 0.45). Increased loadability helps both to increase the production of cheaper generators and decrease wind curtailment at bus $s102$. An additional benefit is a decreased reactive power flow through line $l4$.

Voltage deviations at buses $s102$ and $s104$ are shown in in Fig. 7. Voltage magnitudes at bus $s102$ are slightly decreased after TCSC installation, while the opposite effect is observed at bus $s104$. In periods of lower power flows, i.e. during the first 8 hours and during the night, voltage

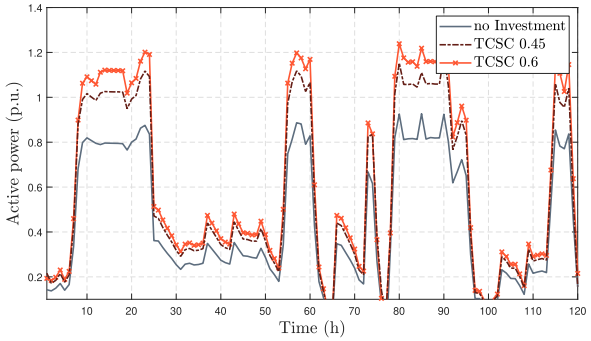

FIGURE 6. Compensation effects of TCSC on power transfer through line *l*4.

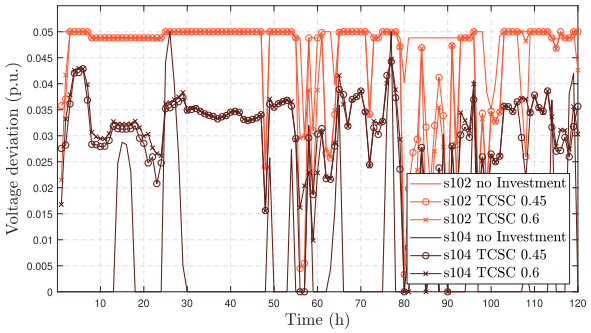

FIGURE 7. Voltage effects of TCSC installed at line *l*4 (buses *s*102–*s*104).

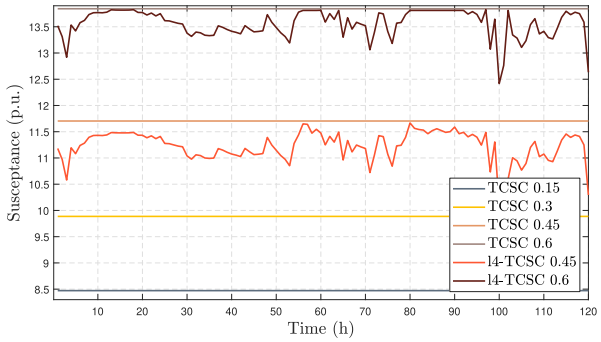

FIGURE 8. Change of susceptance of TCSC installed at line *l*4 considering compensation levels 0.45 and 0.6.

magnitudes are higher because of the low consumption and increased reactive power flows.

Dynamic change of susceptance of TCSC installed on line *l*4 is shown in Fig. 8. The TCSC susceptance changes over time in the subproblem within the range set in the master problem to optimally distribute power flows and affect voltage levels. Correlation between voltage magnitudes, BES operation at bus *s*102 in *low.all* option, and TCSC operation at line *l4* in *low.flex* option is shown in Fig. 9. A representative day in which production of the local wind farm is high during the night is shown. This highly affects the charging schedule of BES, as it charges during the first six hours and discharges as necessary until hour 18. Reactive power is controlled by the BES's converter in order to reduce overall reactive power

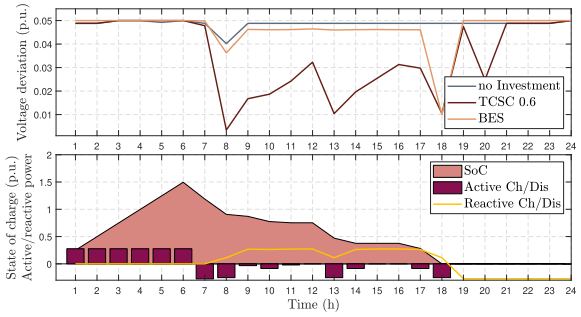

FIGURE 9. Voltage magnitude when BES is installed at bus *s*102 in *low.all*, and TCSC at line *l*4 in *low.flex* option.

flows and losses in the surrounding network while preserving voltage deviations within the given range.

IV. CONCLUSION

This paper proposes a mathematical formulation of the TEP problem considering investments in flexible devices (BES and TCSC) and power lines using a linearized form of AC OPF. The novelty of the paper is the possibility of continuous adjustment of power line reactance in the subproblems (operational problem) after the optimal size of TCSC is determined in the master problem while preserving linearity of the model. Additionally, the paper considers BES providing reactive power control instead of only active power arbitrage. The results of the case study indicate that for the current prices of BES and TCSC, investment in new line is still the most attractive option. However, for lower BES costs, the model results in BES installations at multiple buses, reducing the wind curtailment, but also taking part in voltage control. Investment in TCSC is less attractive and yields lower returns than the investment in new lines. However, it also complements the BES and can come handy at locations where installation of new lines is not possible.

ACKNOWLEDGMENT

The sole responsibility for the content of this document lies with the authors. It does not necessarily reflect the opinion of the Innovation and Networks Executive Agency (INEA) or the European Commission (EC). INEA or the EC are not responsible for any use that may be made of the information contained therein.

REFERENCES

[1] B. Dandrade, *The Power Grid: Smart, Secure, Green and Reliable*. New York, NY, USA: Academic, 2017.
[2] *Renewables 2018-Global Status Report*, REN21, Paris, France, 2018.
[3] R. M. Mathur and R. K. Varma, *Thyristor-Based FACTS Controllers for Electrical Transmission Systems*. Hoboken, NJ, USA: Wiley, 2002.
[4] M. Miletić, Z. Luburić, I. Pavić, and T. Capuder, "A review of energy storage systems applications," in *Proc. MEDPOWER*, Dubrovnik, Croatia, 2018, pp. 1–6.
[5] A. J. Conejo, E. Castillo, R. Minguez, and R. Garcia-Bertrand, *Decomposition Techniques in Mathematical Programming: Engineering and Science Applications*. Cham, Switzerland: Springer, 2006.
[6] I. De J. Silva, M. J. Rider, R. Romero, and C. A. F. Murari, "Transmission network expansion planning considering uncertainty in demand," *IEEE Trans. Power Syst.*, vol. 21, no. 4, pp. 1565–1573, Nov. 2006.

[7] M. Moeini-Aghtaie, A. Abbaspour, and M. Fotuhi-Firuzabad, "Incorporating large-scale distant wind farms in probabilistic transmission expansion planning—Part I: Theory and algorithm," *IEEE Trans. Power Syst.*, vol. 27, no. 3, pp. 1585–1593, Aug. 2012.
[8] X. Zhang and A. J. Conejo, "Robust transmission expansion planning representing Long- and short-term uncertainty," *IEEE Trans. Power Syst.*, vol. 33, no. 2, pp. 1329–1338, Mar. 2018.
[9] C. Bustos, E. Sauma, S. de la Torre, J. A. Aguado, J. Contreras, and D. Pozo, "Energy storage and transmission expansion planning: Substitutes or complements?" *IET Gener., Transmiss. Distrib.*, vol. 12, no. 8, pp. 1738–1746, 2018.
[10] H. Pandzic, Y. Wang, T. Qiu, Y. Dvorkin, and D. S. Kirschen, "Near-optimal method for siting and sizing of distributed storage in a transmission network," *IEEE Trans. Power Syst.*, vol. 30, no. 5, pp. 2288–2300, Sep. 2015.
[11] T. Qiu, B. Xu, Y. Wang, Y. Dvorkin, and D. S. Kirschen, "Stochastic multistage coplanning of transmission expansion and energy storage," *IEEE Trans. Power Syst.*, vol. 32, no. 1, pp. 643–651, Jan. 2017.
[12] K. Pandžić, H. Pandžić, and I. Kuzle, "Coordination of Regulated and Merchant Energy Storage Investments," *IEEE Trans. Sustain. Energy*, vol. 9, no. 3, pp. 1244–1254, Jul. 2018.
[13] M. Rahmani, G. Vinasco, M. J. Rider, R. Romero, and P. M. Pardalos, "Multistage transmission expansion planning considering fixed series compensation allocation," *IEEE Trans. Power Syst.*, vol. 28, no. 4, pp. 3795–3805, Nov. 2013.
[14] F. Ugranli and E. Karatepe, "Coordinated TCSC allocation and network reinforcements planning with wind power," *IEEE Trans. Sustain. Energy*, vol. 8, no. 4, pp. 1694–1705, Oct. 2017.
[15] O. Ziaee and F. F. Choobineh, "Optimal location-allocation of TCSC devices on a transmission network," *IEEE Trans. Power Syst.*, vol. 32, no. 1, pp. 94–102, Jan. 2017.
[16] M. B. Shafik, H. Chen, G. I. Rashed, and R. A. El-Sehiemy, "Adaptive multi objective parallel seeker optimization algorithm for incorporating TCSC devices into optimal power flow framework," *IEEE Access*, vol. 7, pp. 36934–36947, 2019.
[17] D. A. Tejada-Arango, S. Wogrin, and E. Centeno, "Representation of storage operations in network-constrained optimization models for Medium- and long-term operation," *IEEE Trans. Power Syst.*, vol. 33, no. 1, pp. 386–396, Jan. 2018.
[18] H. Zhang, G. T. Heydt, V. Vittal, and J. Quintero, "An improved network model for transmission expansion planning considering reactive power and network losses," *IEEE Trans. Power Syst.*, vol. 28, no. 3, pp. 3471–3479, Aug. 2013.
[19] M. Sahraei-Ardakani and K. W. Hedman, "A fast LP approach for enhanced utilization of variable impedance based FACTS devices," *IEEE Trans. Power Syst.*, vol. 31, no. 3, pp. 2204–2213, May 2016.
[20] T. Akbari and M. Tavakoli Bina, "A linearized formulation of AC multi-year transmission expansion planning: A mixed-integer linear programming approach," *Electric Power Syst. Res.*, vol. 114, pp. 93–100, Sep. 2014.
[21] H. Pandžić, Y. Dvorkin, T. Qiu, Y. Wang, and D. S. Kirschen. Unit commitment under Uncertainty–GAMS Models. REAL Lab Library, University of Washington, Seattle, WA, USA. Accessed: Oct. 1, 2020. [Online]. Available: www.ee.washington.edu/research/real/gams_code.html
[22] N. Growe-Kuska, H. Heitsch, and W. Romisch, "Scenario reduction and scenario tree construction for power management problems," in *Proc. IEEE Bologna Power Tech Conf.*, Bologna, Italy, 2003, pp. 1–7.
[23] M. Carrion, Y. Dvorkin, and H. Pandzic, "Primary frequency response in capacity expansion with energy storage," *IEEE Trans. Power Syst.*, vol. 33, no. 2, pp. 1824–1835, Mar. 2018.
[24] N. Acharya and N. Mithulananthan, "Locating series FACTS devices for congestion management in deregulated electricity markets," *Electr. Power Syst. Res.*, vol. 77, nos. 3–4, pp. 352–360, Mar. 2007.
[25] L. Cai, I. Erlich, and G. Stamtsis, "Optimal choice and allocation of FACTS devices in deregulated electricity market using genetic algorithms," in *Proc. IEEE PES Conf. Expo*, New York, NY, USA, Oct. 2004, pp. 201–207.
[26] M. J. Rider, A. V. Garcia, and R. Romero, "Power system transmission network expansion planning using AC model," *IET Gener., Transmiss. Distrib.*, vol. 1, no. 5, pp. 731–742, Sep. 2007.

ZORA LUBURIĆ (Member, IEEE) received the M.E.E. degree from the Faculty of Electrical Engineering and Computing, University of Zagreb, Croatia, in 2015, where she is currently pursuing the Ph.D. degree. She was a Research Assistant with the Department of Energy and Power Systems, University of Zagreb, for a period of three years. She is also with the Market Department, Balancing Services, Croatian Transmission System Operator. Her research interests include planning, operation, and economics of power and energy systems.

HRVOJE PANDŽIĆ (Senior Member, IEEE) received the M.E.E. and Ph.D. degrees from the Faculty of Electrical Engineering and Computing, University of Zagreb, Zagreb, Croatia, in 2007 and 2011, respectively. From 2012 to 2014, he was a Postdoctoral Researcher with the University of Washington, Seattle, WA, USA. He is currently an Associate Professor and the Head of the Department of Energy and Power Systems with the Faculty of Electrical Engineering and Computing, University of Zagreb. His research interests include planning, operation, control, and economics of power and energy systems.

MIGUEL CARRIÓN (Member, IEEE) received the degree and the Ph.D. degree in industrial engineering from the University of Castilla–La Mancha, Ciudad Real, Spain, in 2003 and 2008, respectively. He is currently an Associate Professor with the University of Castilla–La Mancha, Toledo. His research interests include planning, operation, and economics of power and energy systems.